INFLUENȚA PARAMETRILOR PROCESULUI DE DEPUNERE CU LASER ȘI A TRATAMENTULUI TERMIC SOLAR ASUPRA PROPRIETĂȚILOR STRATURILOR BIOCOMPATIBILE INCONEL 718

INFLUENCE OF THE LASER CLADDING PARAMETERS AND SOLAR HEAT TREATMENT ON THE PROPERTIES OF BIOCOMPATIBLE INCONEL 718 COATINGS

ALEXANDRU PASCU[1], E.M. STANCIU[1], IONUȚ C. ROATĂ[1], IOSIF HULKA[2]*, DRAGOȘ UȚU[2], IOANA MAIOR[3]*

[1] *Transilvania University of Brasov, 29 Eroilor Blvd., 500036, Braşov, Romania*
[2] *Politehnica University Timisoara, 2 Piaţa Victoriei, 300006 Timişoara, Romania*
[3] *University POLITEHNICA Bucharest, Inorganic Chemistry, Physical Chemistry and Electrochemistry Department, 1-7 Polizu Str., 011061 Bucharest, Romania*

The paper presents the influence of the deposition process parameters in order to obtain dense and no major defect biocompatible alloys based on Inconel 718 hard coatings deposited on AISI 5140 carbon steel substrate using laser cladding method. Moreover, the cladded coating properties under optimal manufacturing conditions in terms of microhardness and tribological behaviour were improved by surface solar energy irradiation. The microstructure of the Inconel 718 coating before and after solar heat treatment was investigated by scanning electron microscopy (SEM) and the sliding wear resistance was determined by pin-on-disk method (POD).

Lucrarea prezintă influenţa parametrilor de depunere în scopul obținerii de aliaje biocompatibile dense şi fără defecte majore, bazate pe acoperiri dure de Inconel 718, depuse prin placare cu laser pe suprafața unui oțel AISI 5140 folosit ca substrat. Mai mult decât atât, proprietățile stratului depus în condiţii optime, privind duritatea şi comportamentul tribologic, au fost îmbunătățite prin tratament termic de suprafață, folosind ca sursă de iradiere energia solară. Microstructura straturilor Inconel 718 înainte și după tratamentul termic a fost investigată prin microscopie electronică de baleiaj (SEM), iar rezistența la uzură a fost determinată prin metoda pin-on-disk (POD).

Keywords: *biocompatible coatings, laser cladding, solar heat treatment, wear resistance*

1. Introduction

In recent years a growing interest of researchers in developing new manufacturing techniques for biocompatible metallic materials with high corrosion and wear resistance has been noticed [1–6].

In this regard, the applicability of laser cladding to the fabrication of biomedical devices from hard coatings on carbon steel substrates was investigated [1–6].

Implanted metallic medical devices must fulfil certain criteria: compatibility with the biological environment, perfect operation for a long time, mechanical and chemical resistance in contact with human body tissues [1, 2, 4–6].

To achieve these features a significant attention has been given to improving processes and finding the optimum processing parameters in manufacturing metallic biomedical devices knowing that processing can be used to accurately engineer the surface characteristics (wear, corrosion and fatigue resistance) by inducing compressive residual stress and hard surface coatings [1 – 6].

In our previous work [3], laser cladding NiCrBSi composite coatings deposited on the surface of stainless steel substrates has been shown to enhance the relevant functional characteristics of biomaterials such as the microstructure and wear resistance. The key mechanism by which these improvements are performed is monitoring and control of the heat generated during processing, which leads to thermal minor surface and sub-surface defects comparing to conventional manufacturing techniques.

During last decades laser cladding has become a common process used for enhancing or reconditioning of wear components. Coatings are realized by using the laser beam as heating source and a feedstock material in the form of wire or powder. Both material used as feedstock options

* Autor corespondent/*Corresponding author*,
E-mail: iosifhulka@upt.ro, maior_i@yahoo.com

have advantages and disadvantages like adding or varying the alloy chemistry. This is an easy task in case of powders. One of the feedstock powders used in laser cladding is Ni-based obtained through gas atomization and it has the widest range of application where superior corrosion and high wear resistance are demanded [7]. The Inconel 718 is a precipitation hardenable Ni-Cr-Fe austenite alloy with a high corrosion resistance, excellent creep rupture strength at high temperature and good tensile, fatigue, rupture strength favourable weldability. Due to these characteristics is frequently used in applications for aerospace, pollution control equipments, power plants, etc. [8–10]. Even if the alloy presents very low carbon content several problems may occur during laser cladding. Due to the high thermal gradient micro-cracks, pores and coarse dendrite structure may affect the quality of the Inconel coating [11]. Zhong et al. [12] identified five styles of boundary liquation and interface cracking at Inconel 728 laser cladded on a Ni-based super-alloy. Though, as related [12, 13] the process parameters optimizations may provide cracks free Inconel layers. The Inconel grade is well known in engineering for long time but the speciality literature is limited in the case of laser cladding of this material. Using new type of lasers and optics may be the solution to eliminate the down-backs induced by the thermal processing of this alloys [14, 15]. Parimi et al. [11] uses a continuous wave fibre laser to deposit IN718 powder and reports the presence of defects like porosity, un-melted powder and metal liquation cracking in the coating. Baldridge et al. [16] uses an high power Yb fibre laser to obtain successful multilayer cladding of Inconel 690 with minimal porosity and surface defects. Several studies [17–19] have been reported that optimization of the laser cladding parameters in case of Inconel alloys is the best method to decrease the liquation cracking susceptibility. Moreover a right balance between power, speed and feed rate will ensure a fine and uniform microstructure. A solution in this direction is not been established yet because the process parameters are related with the equipment used (e.g. laser wavelength, beam geometry, focusing optics). As reported by Parimi et al. [11] the liquation cracks may be healed after a post-clad heat treatment. The effects of heat treatment on the microstructures and mechanical properties of composite coatings have been widely investigated and the results demonstrated that some unwanted defects (like pores) of composite coatings can be reduced and in the meantime the hardness can be improved by heat treatment [20].

In the present study laser cladding using MetcoClad 718 powder and various process parameters in order to deposit single tracks was performed. The obtained tracks were studied in cross-section in order to determine track geometry, microstructure and composition. The influence of process parameters on the clad track characteristics was investigated. Optimal process parameters were identified for coatings manufacture. The single tracks and coatings were cladded on AISI 5140 carbon steel substrate. Moreover, the influence of the surface solar energy treatment of the laser cladded coating on the microhardness and sliding wear behaviour were studied. A Heliotron solar reactor was used as green energy to convert the solar light into heat, the concentrated light being used as irradiation source for the Inconel coatings.

2. Materials and methods

2.1 Materials

Self-fluxing Inconel 718 powder (Fig. 1b) supplied by Sulzer Metco as MetcoClad 718 (Inconel 718) was used to obtain the laser single tracks and furthermore optimised coating on AISI 5140 steel substrate. The chemical composition of the substrate and feedstock powder is presented in Table 1 and Table 2, respectively.

Table 1

Chemical composition of the base material / *Compoziția chimică a materialului de bază*

Substrate / Substrat	**Element / *Element* [wt. %] / [% grav.]**									
	C	**Cr**	**Si**	**Ni**	**Fe**	**Mn**	**S**	**Mo**	**P**	**Cu**
AISI 5140 steel / oțel	0.364	0.98	0.223	0.096	97.5	0.65	0.021	0.019	0.013	0.13
	Al	**Co**	**Ti**	**N**	**B**	**Nb**	**Sn**	**V**	**W**	**Pb**
	0.026	0.0066	0.0006	0.017	0.0007	0.0033	0.0080	<0.0039	<0.0070	<0.0020

Table 2

Chemical composition of Ni based powder (according to the manufacturer)
Compoziția chimică a pulberii pe bază de Ni (conform producătorului)

Material	**Element / Element [%]**											**Powder dimension / Dimensiunea particulelor [µm]**
	Ni	**Cr**	**Fe**	**Mo**	**Cu**	**Nb**	**Ti**	**Si**	**Mn**	**C**	**B**	
MetcoClad 718	bal	19	18	3	-	5	1	0.2	0.08	0.05	0.005	-90 ÷ +44

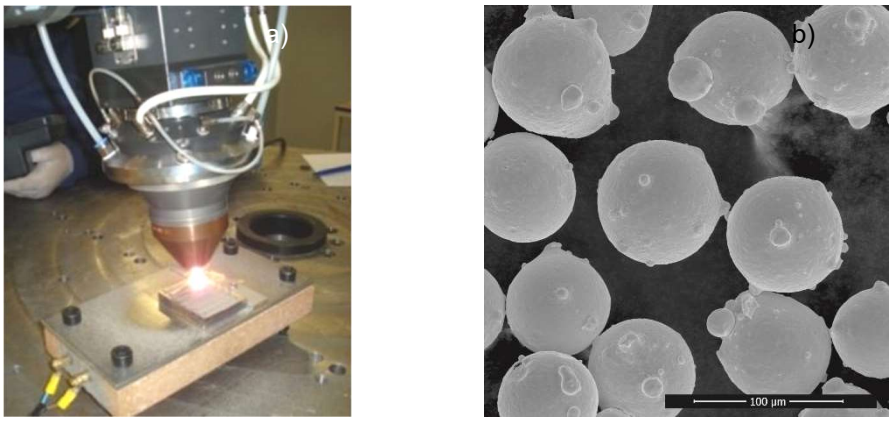

Fig 1 - (a) Experimental frame used for the laser cladding, (b) SEM microscopy of the Inconel 718 powder.
(a) Cadrul experimental utilizat pentru depunerile cu laser, (b) Microscopie SEM a pulberii Inconel 718.

Table 3

Experimental conditions and response factors for laser cladding process
Parametrii operaţionali şi factorii de răspuns ai procesului de depunere cu laser

Specimen / Parameters	Sample 1 Proba 1	Sample 2 Proba 2	Sample 3 Proba 3	Sample 4 Proba 4	Sample 5 Proba 5	Sample 6 Proba 6	Sample 7 Proba 7	Sample 8 Proba 8
Laser power / *Putere laser* [W]	600	650	700	750	800	850	900	950
Power density / *Densitate putere* [kW/cm^2]	19.1	20.7	22.3	23.8	25.4	27.0	28.6	30.2
Powder feed rate / Debit alimentare pulbere [g/min]	40							
Cladding speed / *Viteză depunere [mm/s]*	5							

2.2. Laser cladding

A coaxial laser cladding (Fig. 1a) was used to produce single tracks of Inconel 718 on AISI 5140 steel substrate using different heat powers. The experiments were carried out using a Coherent F1000 diode laser together with Precitec WC 50 cladding head manipulated by a CLOOS welding robot. The powder was provided to the cladding head with AT-1200HPHV Termach feeding system and Argon was used as shielding gas and as carrier gas for the powder. Tilting of the cladding head at 3º in the cladding direction and defocused laser beam of 2 mm was used for all the cladding tests. The standoff distance was set at 12.5mm.

In order to optimize the cladding parameters 8 single tracks of 80 mm were cladded with adjusted laser power in the range of 600-950 W and adjusted power density at constant scanning speed of 5 mm/s and 40 g/min powder feeding rate. In laser cladding deposition, the microstructural properties and phase composition of the coatings are significantly affected by laser power, laser power density, cladding speed and powder feed rate, as results from the following equation:

$$LPD = \frac{P}{\frac{\pi D^2}{4}} \qquad (1)$$

where LPD is the laser power density, P is the laser power and D is the laser beam diameter.

Therefore the laser power density increases as the laser power is increased [21].

The laser cladding parameters and the main geometrical dimension are summarised in Table 3.

2.3. Heat treatment process

Furthermore, to improve the properties of the deposited coating resulted using the optimized laser track cladding parameters, a surface solar energy treatment was used.

The Heliotron solar furnace, used as heating source, is one of the twelve furnaces at PRONES (Solar facilities at Odeillo, CNRS, France) and it is made out of mobile plane mirrors which capture the sun radiation and reflect it toward a parabolic concentrator.

The parabolic mirrors focus the light on the reactor which is made of a glass balloon in which the solar radiation is focused toward the coated sample as presented schematically in Figure 2. Inside the glass balloon the reaction can take place under an inert gas thus the atmosphere being controlled [22]. The concentrated sun radiation could rich 1kW of thermal power at a minimum spot diameter of 2 cm. This method was chosen due to the low environmental impact of the energy generated by the sun and also because of the concentrated heating source which made possible the surface treatment of only the coated Inconel 718 coating preserving in the meantime the substrate at

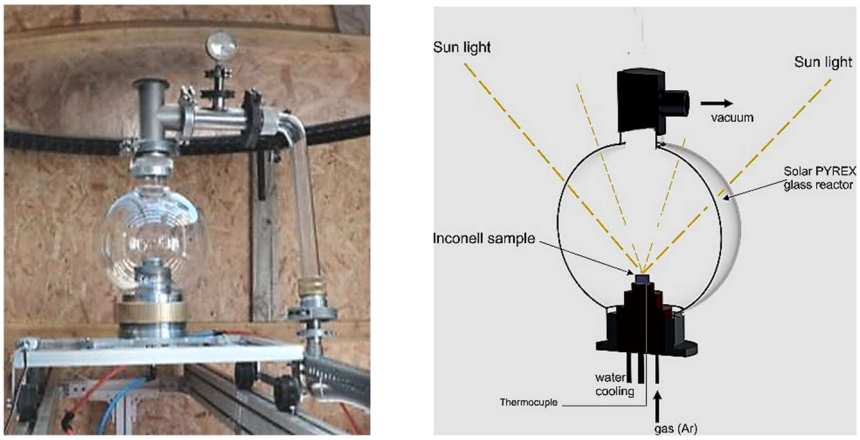

Fig. 2. - Experimental set-up used for the solar heat treatment: a) schematic representation, b) solar reactor.
Cadrul experimental utilizat pentru realizarea tratamentelor termice, a) reprezentare schematică, b) cuptorul solar

a lower temperature. The samples were positioned on o water cooled plate in order to maintain a low temperature of the base material (250 – 320 °C). The temperature was measured by means of a thermocouple system.

The solar heat treatment was performed at 980 °C during 3.5 h period time in low vacuum (55 hPa pressure) using a constant Argon flow of 1 L/min. The cooling of the sample was performed in air at 300ºC / hour.

2.4. Material characterization and properties evaluation

The samples were prepared for metallographic inspection by electrochemical etching in solution of 10% oxalic acid.

The morphologies and microstructures of the single tracks and coatings were studied by scanning electron microscopy (SEM) including EDX (Quanta FEG 250, equipped with EDAX analyzer – FEI). The dilution of single cladded tracks was studied using an Olympus GX51 optical microscope.

The microhardness of the coatings was measured using a Shimadzu HMV 2T microhardness tester. Ten HV02 indentations on each specimen were performed with the following set-up: load 200gf and dwell time of 15 sec; the average value was calculated for each cladded track and coating. The morphologies of the laser cladded tracks were characterized in cross-section by SEM (Quanta FEG 250 - FEI) equipped with an energy dispersive spectrometer.

The coating deposited using the optimized laser track cladding parameters before and after the heat treatment were also metallographically prepared and investigated by mean of optical and SEM microscopy. The samples have been analysed in cross-section and also on the top surface after removing by grinding 1/3 from coating surface.

To evaluate their wear properties a ball-on-disk tribometer from Ducom Instruments was used. For that, the samples were grinded and polished till a mirror like surface was obtained. As counterpart a WC ball with a 6 mm diameter was used. The testing conditions were as following: applied load of 10N, wear diameter 9 mm, testing time 127 min and 1000 m sliding distance. The wear tests for each coating were repeated three times to provide the reproducibility of the experimental result. The morphologies of the worn surfaces were characterized using a Quanta FEG 250 (FEI) equipped with an energy dispersive spectrometer. The wear rate was determined using a 3D optical profilometer (Ducom Instruments).

3. Results and discussions

3.1. Effect of process parameters on clad geometry characteristics, dilution and microstructure

In order to evaluate the influence of the laser heating power on the cladded microstructure, the main geometrical dimensions and the calculated dilution values were determined (Table 4).

Figure 3 shows the macro appearances of the deposited Inconel 718 individual tracks. It can be observed that all tracks have similar profiles with small modification regarding geometrical dimensions. The height and clad area of single tracks are influenced by the laser power directly due to the amount of melted powder. As the laser power increases more material is melted. Moreover the dilution increases at high power due to higher ratio between the clad area and the molten area. Therefore dilution can be defined as the ratio of the clad depth in the substrate to the sum of the clad height, above the substrate surface, and clad depth. Dilution determines the amount of liquid layer that needs to be formed on the substrate to ensure layer bounding. It is the change in composition of the clad material due to mixing with the substrate material during melting and is generally required to keep it at low levels [23]. By using a defocused laser beam was possible to maintain a low molten area and to increase the quantity of deposited powder.

Table 4

Laser cladded single tracks characteristics / *Caracteristicile cordoanelor depuse cu laser*

Specimen / *Probă*	**Sample 1** ***Proba 1***	**Sample 2** ***Proba 2***	**Sample 3** ***Proba 3***	**Sample 4** ***Proba 4***	**Sample 5** ***Proba 5***	**Sample 6** ***Proba 6***	**Sample 7** ***Proba 7***	**Sample 8** ***Proba 8***
Clad high / *Înălțimea placării* h_d [µm]	0.343	0.422	0.383	0.40	0.433	0.521	0.446	0.432
Clad area / *Aria placării* Ac [mm^2]	0.38	0.50	0.50	0.58	0.65	0.85	0.73	0.81
Clad width / *Lățimea placării* L [µm]	1.638	1.781	1.913	2.09	2.20	2.32	2.48	2.69
Melt depth / *Adâncimea topiturii* p_d [µm]	0.13	0.151	0.170	0.191	0.200	0.206	0.241	0.292
Molten area / *Aria topiturii* Am [mm^2]	0.19	0.21	0.28	0.35	0.40	0.42	0.56	0.69
HAZ area / *Aria* HAZ [mm^2]	1.21	1.34	1.60	1.82	2.18	2.31	2.54	2.91
Wetting angle / *Unghiul de udare* α [º]	141	135	145	148	146	138	150	147
Dilution / *Diluare* [%]	29.6	33.1	33.3	35.9	37.6	38.1	43.4	46.0

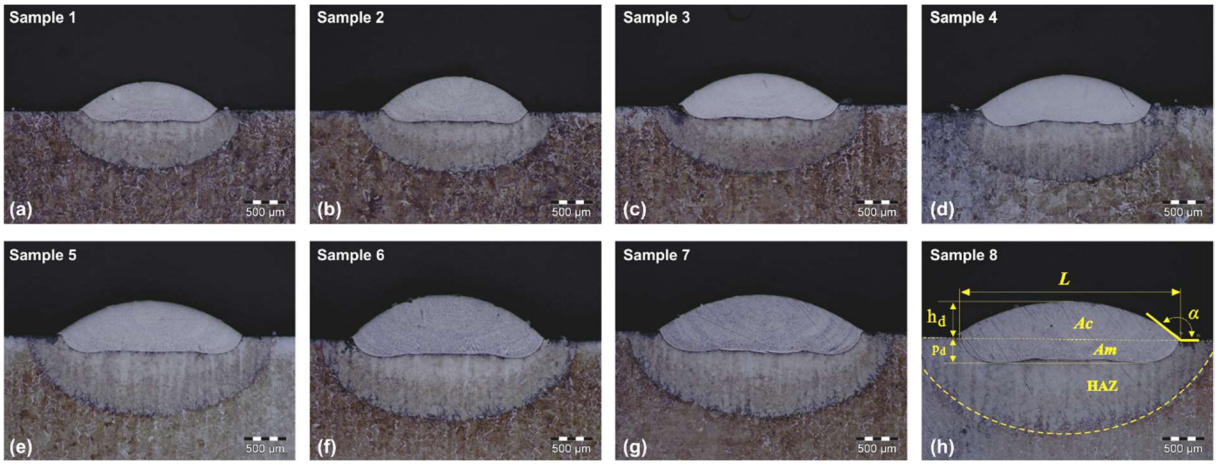

Fig. 3.- Low magnification of laser cladded single tracks in cross-section for all samples, (h) geometrical profile of the cladded track
Secțiunea depunerilor cu laser și pulbere pentru toate probele, (h) profilul geometric al cordoanelor depuse.

Analysing Table 3 and 4 it might be noticed an increase of the clad profile and heat affected zone if the laser power reaches to higher values. Also, dilution is more pronounced. Dimensionally, the thickness of the diffusion area (non-interference zone) increases along with the growing of the power amount used, namely, from 1.1 µm at 600 W up to 1.9 µm at 950W. Also, at high power densities, the emergence and emphasis of dendrite structures were noticed.

The two materials (cladded material and substrate) are separated by a well-defined non-interference line. The solidification pattern is determined by the thermal gradient induced by the laser. Hence, by varying the laser power different morphologies of the dendrite and precipitated phases were achieved.

Beside the thermal gradient, the dilution has a crucial role in the formation of the clad microstructure. According to EDX quantification presented in Figure 4 and Table 5 it can be seen that nearby the boundary zone there is a higher concentration of iron which was transferred from the base material. As the investigated area is closer to the upper part of the clad, the chemical composition is similar with the powder composition. From EDX analyses made on all samples, was observed that iron is still present in high concentration in all the clad area. Even in the upper part of the cladded track the iron concentration was found to be 39 wt.% in case of sample 4 and 47 wt.% in case of sample 8 which was cladded with the highest laser power. It was determined that the iron concentration in the cladded layers is almost double compared to the powder composition. A high content of iron can decrease the corrosion resistance of the cladded layers.

Due to similar morphologies of the cladded tracks only the characteristics of sample 4 are discussed down below.

In Figure 5 it can be seen that different precipitated phases are formed in the primary γ Ni solution. It is thought that these interconnected precipitated phases form hexagonal patterns which enclose the Ni solution (Figure 5a). Round shape phases presumably Ni_3Nb-δ, Nb-rich MC carbides and lava phases are present in the hexagonal pattern (Figure 5b). The lava phases are form due to the Nb segregation and according to the literature [11, 24] have a typical chemistry of $(Ni, Fe, Cr)_2(Mo, Nb, Ti)$. This type of brittle lavas segregation has a detrimental impact on the microhardness of the cladded tracks. Moreover,

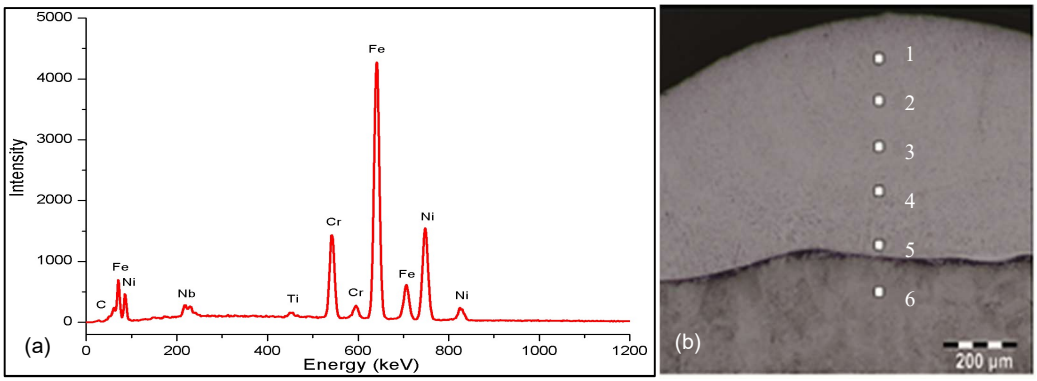

Fig. 4- EDX spectrum in cross-section of sample 4 cladded track (a) and EDX analysed micro-areas in cross-section on sample 4 (b). *Spectrul EDX al probei 4 în secţiune (a) şi distribuţia microzonelor analizate EDX (b)*

Table 5

EDX quantification of micro-areas indicated in Figure 4b

Distribuția procentuală a elementelor de aliere în secțiunea cordonului conform Figurii 4b

Element / Microzone	Nb [wt %]	Mo [wt %]	Ti [wt %]	Cr [wt %]	Fe [wt %]	Ni [wt %]
Microzone 1	6.5	4.7	0.8	15.5	33.5	39.0
Microzone 2	4.8	4.5	1.1	11.3	37.5	40.8
Microzone 3	3.5	2.1	0.6	12.5	47.1	34.2
Microzone 4	1.1	1.5	0.7	8.7	57.4	30.6
Microzone 5	2.1	0.8	0.3	4.3	76.8	15.7
Microzone 6	1.6	0.8	0.1	1.3	93.9	2.3

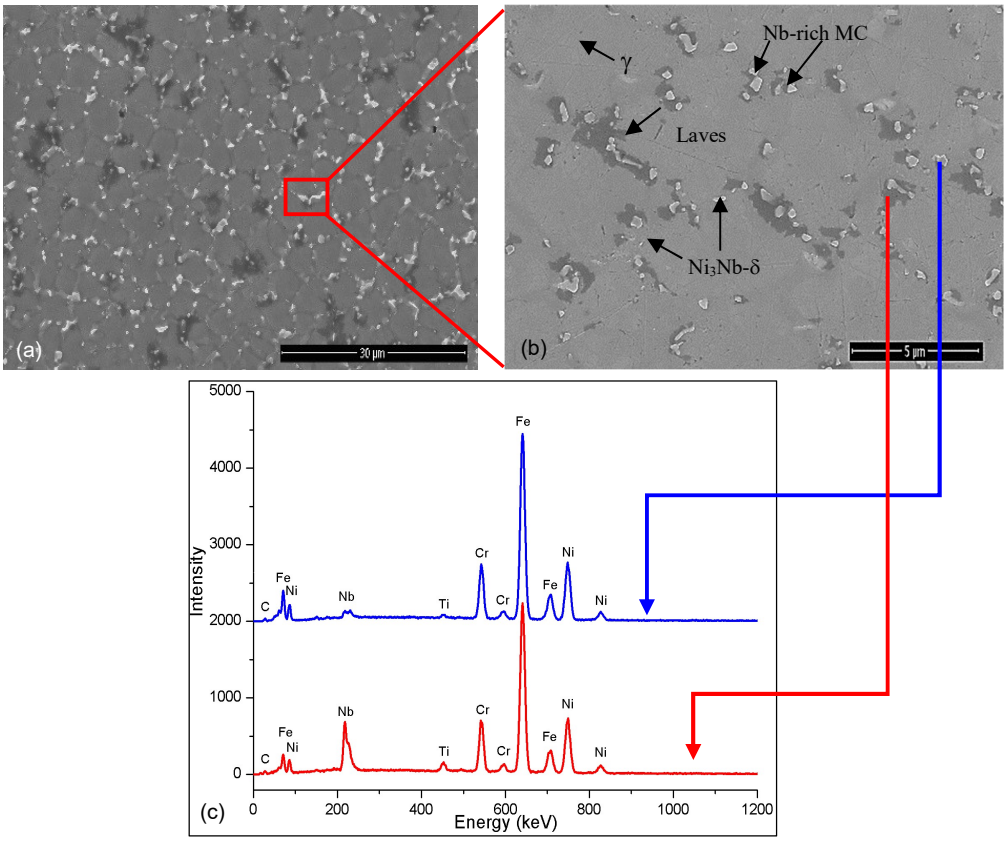

Fig. 5 - SEM micrograph of precipitated phases synthesized (a); high magnifications of the precipitation formation with a high niobium content and lavas phases (b); EDX spectrum of hard phase particles and its surrounded region (c) / *Micrografie SEM a fazelor precipitate sintetizate (a); detaliu al formării precipitatelor cu un conținut ridicat de niobiu şi a fazelor lava (b); Spectrul EDX al unei particule dure şi al zonei din proximitatea acestuia (c).*

the Nb segregation combined with the rapid solidification occurred at laser processing could promote the crack initiation at grain boundary. Each Nb carbide is surrounded by a dark area. The EDX analyses (Figure 5c) reveal that the irregular shaped particle is rich in Nb and the surrounded area has a high concentration of iron.

This segregation pattern it is thought to be more pronounced near the interface with the substrate where a high amount of iron is transferred from the base material.

The hardness was determined using a micro-Vickers hardness tester under the maximum indentation load of 200 g ($HV_{0.2}$) equivalent to 1.961 N testing force. Figure 6 presents the hardness values of the Inconel 718 single cladded tracks depending on the laser power. It can be noticed that hardness decreases along with the increase of the laser power used in the process. The hardness decreases due to the increased dilution percentage between the materials and by the different crystallization and segregation pattern promoted by the gradient temperature. At low laser powers the powder formed fine and dimensionally uniform dendrite structures with small amount of laves and precipitation formation presented in Figure 5.

It must be taken into account that in case of coating formation by partially overlapped tracks, the melted zone area will remain constant after cladding the first layer, then for the following layers the cladding thickness will increase without influencing the melting depth. Thus, dilution will be considerably reduced, and it will decrease up to 10-15% in case of partially overlapped tracks during the deposition of new coatings.

In order to obtain the coating, partially

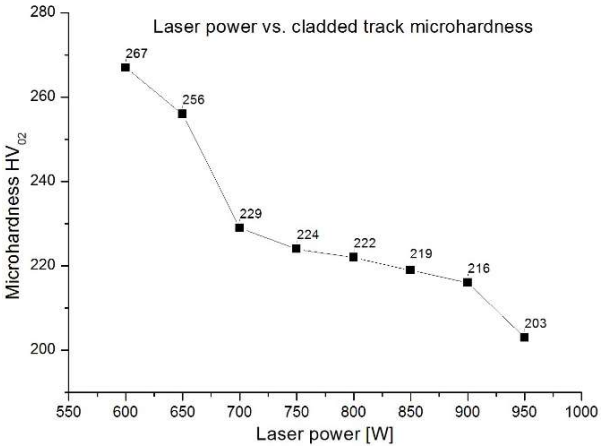

Fig. 6- Dependence between the laser power and the microhardness of single cladded tracks / *Dependența dintre puterea laserului și microduritatea cordoanelor*

overlapped tracks were realised by coaxial laser cladding using the chosen parameters determined from the single track experimental tried-out for sample 4. The chosen parameters were used as a function of microhardness and lower segregation compared to samples 5 – 8 which present a pronounced modification in the chemical composition due to an increased dilution. As the laser power increases the microhardness decreases significantly due to an increased Fe content within the cladded tracks. Sample 4 presents an average hardness value which it is thought that is suitable for the coatings because it does not present an increased dilution and it does not present the highest hardness values which could do the coatings more fragile. Laser cladding

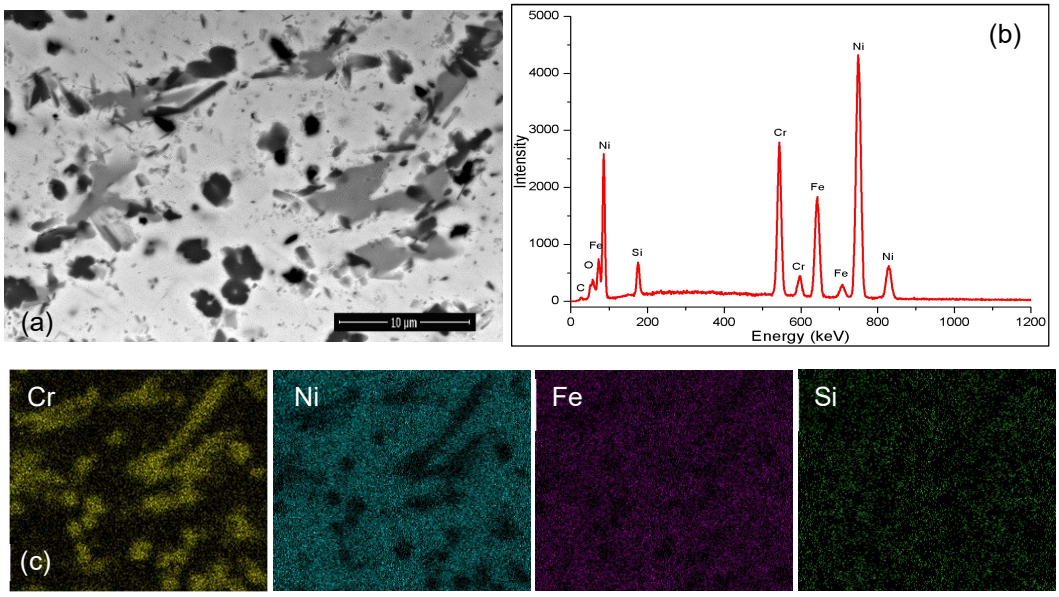

Fig. 7 - SEM micrograph of solar heat treated sample (a), afferent EDX spectrum (b) and EDX mapping of Inconel 718 coating after solar heat treatment / *Micrografie SEM a stratului tratat termic cu energie solară (a), spectru EDX aferent şi mapare EDX a stratului Inconel 718 după tratamentul termic solar.*

with Inconel 718 alloy on 16 mm AISI 5140 carbon steel plate have been obtained using the same experimental setup and adding the specific parameters, respectively the overlapping degree and number of tracks. The cladding of the coating was performed using 750 W laser power at 22 cm/min speed rate with a powder feed rate of 5 g/min. The overlapping degree was 45% and the stand-off distance 12 mm.

Because Inconel 718 is a precipitation hardenable superalloy, after coatings deposition by laser cladding overlapping, some of the samples were surface treated using the Heliotron solar furnace. At high magnification both coatings, in as-cladded state and after heat treatment, presented similar microstructure. As an example it has been chosen the microstructure and its afferent EDX spectra of surface treated coating presented in Figure 7. The SEM micrograph (Figure 7a) revealed a dense cladded coating indicating that the feedstock powder was melted completely.

For elements distribution, according to EDX mapping (Figure 7c), the dark and grey areas are Cr rich regions. Apart from Cr it has been noticed that Ni, Fe and Si, which are the main constituents of the matrix, are homogenously distributed within the coating. One can also observe the absence of Nb which probably formed new hard phases during the cladding process and heat treatment.

3.2. Microhardness and tribological properties of Inconel 718 coatings

It has been found that solar irradiation enhanced the hardness of the cladded coatings (increased from 215 HV_{02} to 438 HV_{02}) as presented in Table 6. The higher values are probably due to the precipitation hardening phenomena and because of the lava phase reduction from the metal matrix. The differences regarding the hardness values between the cladded track and as-cladded coating deposited with optimal parameters is attributed to different cooling rates; during cladding the cooling rate is lower because every new deposited track warms up the previous deposited track which decrease the final coating hardness.

The wear results obtained at room temperature in dry conditions for as-deposited and solar heat treated Inconel 718 laser cladded coatings are presented in Table 6.

Wear of the cladded coatings is influenced by abrasion and adhesion. During ball-on-disk fine debris were entrapped between the surface and counter-body acting as abrasive media (dark areas on the surface presented in Figure 8a). According to these results the lowest coefficient of friction and wear rate were attributed to the surface treated coating. The results were in correlation with the obtained hardness values so thus, one may suppose that the better wear resistance might be attributed also due to the precipitation hardening phenomena and reduction of the lava phase from the metal matrix.

Due to similar wear track morphology only the heat treated sample was presented in Figure 8 of which it can be observed that the damaged surface of Inconel 718 samples present adhesion, spalling and oxidation according to the afferent EDX spectrum. Furthermore, delaminating damage might be noticed on the wear surfaces and also the samples were subjected to plastic deformation.

Table 6

Results of pin-on-disk measurements / *Rezultatele măsurătorilor pin-on-disk*

Sample / *Probă*	Microhardness *Microduritate* [HV_{02}]	C_oF [μ]	Wear index / *Indice de uzură* [$mm^3/N \cdot Km$]
ASC (as-cladded coating) *ASC (depunere cu laser)*	215	0.563	648.931
STT (after heat treatment) *STT (după tratamentul termic)*	438	0.489	383.563

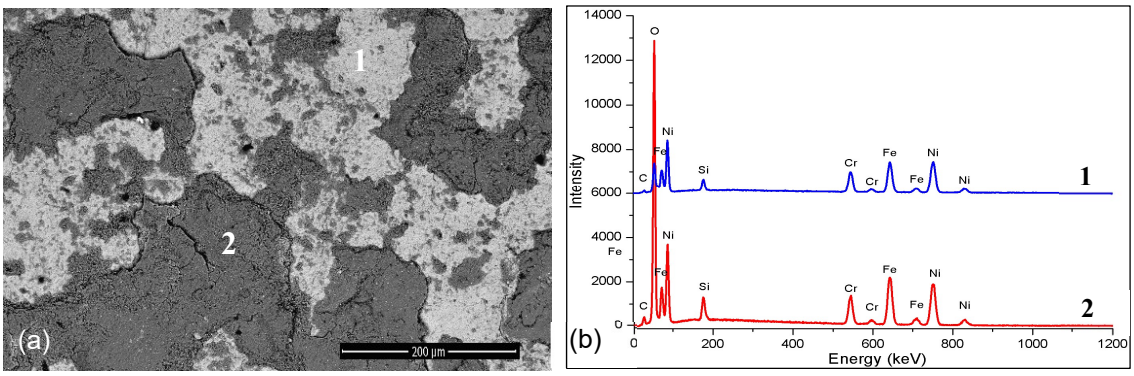

Fig. 8 - SEM micrograph (a) and afferent EDX spectrum (b) of wear scar produced on Inconel 718 laser cladded coating after solar heat treatment / *Micrografie SEM a urmei de uzură produsă pe proba STT (a) şi spectrele EDX ale diferitelor zone (b).*

4. Conclusions

The geometry, microstructure, chemistry and microhardness of the Inconel 718 deposited by laser cladding were evaluated for single tracks, as-deposited cladded coating and after the surface treatment using solar energy. The following conclusions were acquired from the exposed experimental investigation:

– cracks and pore free Inconel 718 coatings may be produced using laser cladding technology;

– the laser power variation had a direct influence on the clad height, melt depth and dilution; the obtained single track depositions were in all cases dense;

– severe grain boundary segregation was observed in all cladded tracks. A segregation phenomenon was observed. Nb and Ti hard phases precipitated at the grain boundary of cladded tracks. This segregation pattern was more pronounced near the interface with the substrate where a high amount of iron was transferred from the base material;

– growing the laser power the hardness of the single tracks decreases because of the increased dilution percentage between the materials;

– the surface solar treatment of the optimised deposited coatings had a positive influence on the microhardness and tribological behaviour.

Inconel 718 laser cladded coatings followed by solar heat treatment might be an alternative to the manufacture of biomedical devices with increased wear resistance.

Acknowledgements

Financial support by the Access to Research Infrastructures activity in the 7th Framework Programme of the EU (SFERA 2 Grant Agreement n. 312643) is gratefully acknowledged for the access to solar reactors.

References

1. K. Colic, S. Petronic, A. Sedmak, A. Milosavljevic, Z. Kovacevic, Laser Welding Process of Stainless Steel Used for Biomedical Applications, in Proceedings of The 5th International Conference – Innovative Technologies for Joining Advanced Materials, Timişoara, România, June 16-17, 2011, **3**, 16, ISSN 1453-0392.
2. I.S. Jawahir, D.A. Puleo, J. Schoop, Cryogenic Machining of Biomedical Implant Materials for Improved Functional Performance, Life and Sustainability, Procedia CIRP Conference on High Performance Cutting 2016, **46,** 7.
3.. I. Hulka, V.A. Şerban, D. Uţu, N.M. Duţeanu, A. Pascu, I. Roată, I. Maior, Wear Resistance of Laser Cladding NiCrBSi Composite Coatings, Rom. J. Mat., 2016, **46** (1), 424.
4. T.E. Abioye, D.G. McCartney, A.T. Clare, Laser Cladding of Inconel 625 Wire for Corrosion Protection, J. Mat. Processing Techn., 2015, **217**, 232.
5. R. Vilar, A. Almeida, Laser Surface Modification of Biomaterials – Techniques and Applications, **2016**, 35–75, Chapter 2 – Laser Surface Treatment of Biomedical Alloys, Woodhead Publishing Series in Biomaterials: Number 111, Edited by Rui Vilar, ISBN 978-0-08-100883-6.
6. M. Munsch, Laser Additive Manufacturing – Materials, Design, Technologies, and Applications, **2017**, 399–420, Chapter 15 – Laser additive manufacturing of customized prosthetics and implants for biomedical applications, Woodhead Publishing Series in Electronic and Optical Materials: Number 88, Edited by Milan Brandt, ISBN 978-0-08-100433-3.
7. R. J. Lawrence, D Waugh, Laser Surface Engineering: Processes and Applications, Woodhead Publishing, ISBN 978-1-78242-074-3, **2015.**
8. M. Ma, Z. Wang , X. Zeng, Effect of Energy Input on Microstructural Evolution of Direct Laser Fabricated IN718 Alloy, Materials Characterization, 2015, **106**, 420.
9. P. Mithilesh, D. Varun, Ajay Reddy Gopi Reddy, K. D. Ramkumar, N. Arivazhagan, S. Narayanan, Investigations on Dissimilar Weldments of Inconel 625 and AISI 304, Procedia Engineering, 2014, **75**, 66.
10. Qingbo Jia, Dongdong Gu, Selective Laser Melting Additive Manufacturing of Inconel 718 Superalloy Parts: Densification, Microstructure and Properties, J. Alloys and Compounds, 2014, **585**, 713.
11. L. Parimi, G. A. Ravi, D. Clark, M Moataz, Microstructural and Texture Development in Direct Laser Fabricated IN718, Materials Characterisation, 2014, **89**, 102.
12. M.L. Zhong, H.Q. Sun, W.J. Liu, X.F. Zhu, J.J. He, Boundary Liquation and Interface Cracking Characterization in Laser Deposition of Inconel 728 on Directionally Solidified Ni-Based Superalloy, Scr. Mater., 2005, **53,** 159.
13. F. Xu, Y. Lv,Y. Liu,B. Xu,P. He, Effect of Heat Treatment on Microstructure and Mechanical Properties of Inconel 625 Alloy Fabricated by Pulsed Plasma Arc Deposition, Physics Procedia 2013, **50**, 48.
14. H.C. Chen, A. Pinkerton, L. Li, Fibre Laser Welding of Dissimilar Alloys of Ti-6Al-4V and Inconel 718 for Aerospace *Applications*, Int. J. Adv. Manuf. Technol., 2011, **52**, 977
15. L. Quintino, A. Costa, R. Miranda, D. Yapp, Welding with High Power Fiber Lasers – A Preliminary Study, Mater. Des., 2007, **28** (4),1231.
16. T. Baldridge, G. Poling, E. Foroozmehr, R. Kovacevic, T. Metz, V. Kadekar, M.C. Gupta, Laser Cladding of Inconel 690 on Inconel 600 Superalloy for Corrosion Protection in Nuclear Applications, Optics and Lasers in Engineering, 2013, **51**, 180.
17. J. Song, Y. Li, J. Fu, Q. Deng, D. Hu, Cracking Behavior of Laser Cladding Forming Nickel Based Alloys, Technology and Innovation Conference, **2009**, p.1, doi 10.1049/cp.2009.1446
18. O. Nenadl, V. Ocelík, A. Palavra, J.Th.M. DeHosson, The Prediction of Coating Geometry from Main Processing Parameters in Laser Cladding, Physics Procedia, 2014, **56**, 220.
19. U. Oliveira, V. Ocelik, Analysis of Coaxial Laser Cladding Processing Conditions, Surface & Coatings Technology, 2005, **197**, 127.
20. B. Li, Y. Gao, J. Jia, M. Han, H. Guo, W. Wang, Influence of Heat Treatments on the Microstructure as well as Mechanical and Tribological Properties of Nicraly-Mo-Ag Coatings, J. Alloys and Compounds, 2016, **696**, 503-510
21. Chi-Sheng Chien, Cheng-Wei Liu, Tsung-Yuan Kuo, Effects of Laser Power Level on Microstructural Properties and Phase Composition of Laser-Clad Fluorapatite/Zirconia Composite Coatings on Ti6Al4 Substrates, Materials, 2016, **9 (5)**, 380.
22. http://www.sollab.eu/promes.html
23. M. R. Boddu, M. Srinivas, G. L. Robert, A. Sanjeev, W. L. Frank, Empirical Modelling and Vision Based Control for Laser Aided Metal Deposition Process, in Proceedings of Solid Freeform Fabrication Symposium, University of Texas, Austin, USA, **2001**, p. 452.
24. H. Qi, M. Azer, A. Ritter, Studies of Standard Heat Treatment Effects on Microstructure and Mechanical Properties of Laser Net Shape Manufactured INCONEL 718, Metallurgical and Materials Transactions A, 2009, **40** (10), 2410.

****